Jurnal Kejuruteraan 32(2) 2020: 307-313
https://doi.org/10.17576/jkukm-2020-32(2)-15

Preliminary Study of Effective Copper Indium Sulfide ($CuInS_2$) Quantum Dots as Photo-sensitizer in Solar Cell

Nurul Syafiqah Mohamed Mustakim[a], Javad Safaei[a], Charles Ahamefula Ubani[a,b], Suhaila Sepeai[a], Norasikin Ahmad Ludin[a], Mohd Asri Mat Teridie[a] & Mohd Adib Ibrahim[a*]

[a]*Solar Energy Research Institute (SERI), Universiti Kebangsaan Malaysia, Malaysia*
[b]*Cahams Research Consultant, Nigeria*
**Corresponding author: mdadib@ukm.edu.my*

Received 17 September 2019, Received in revised form 28 December 2019
Accepted 21 January 2020, Available online 30 May 2020

ABSTRACT

Recent studies showed that quantum dots (QDs) materials such as cadmium (Cd) and lead (Pb) are commonly used as sensitizer in solar cell applications. This is mainly because they have high potential in light harvesting. However, these materials are highly toxicity and very harmful to the environment. Therefore, current investigation reports the performance of quantum dots sensitized solar cells (QDSSCs) based on non-toxicity $CuInS_2$ QDs by using solvothermal process. TiO_2 paste were deposited by doctor blade method on transparent conducting fluorine doped tin oxide (FTO) glass substrates. The $CuInS_2$ nano sized QDs were controlled by different solvothermal reaction times of 2 hours, 4 hours, 6 hours and 8 hours. In this study, the morphology, structural and optical properties of prepared TiO_2/$CuInS_2$ QDs thin films were investigated by using Transmission Electron Microscope (TEM), Atomic Force Microscope (AFM), X-ray Diffraction (XRD) and Ultra-Violet-Visible Near Infrared Spectrophotometer (UV-Vis). The diameter of $CuInS_2$ QDs was found to be increased from 3.19 nm to 8.67 nm with longer reaction time. Results showed that $CuInS_2$ QDs with longer reaction time produced higher conversion efficiency. Based on the experiment done, $CuInS_2$ QDs with 8 hours reaction time produced the best power conversion efficiency; 0.035 %. Regarding the considerable efficiencies obtained, pointed out that $CuInS_2$ QDs can be introduced as an effective photosensitizer for making efficient QDSSCs devices.

Keywords: Copper Indium Sulfide; Non-toxic; Quantum dots; Solar cell; Solvothermal method

INTRODUCTION

In the past few years, QDs have attracted a lot of attention due to their unique and outstanding properties (Liu et al. 2016). Basically, QDs are semiconductors material that have very small particles, between 2 and 10 nanometers in diameter (Hegazy and El-hameed 2014) (Kouhnavard et al. 2014). QDs absorb and emit exact colours at specific wavelengths that correspond to their particle size. In general, larger QDs emit red light, while smaller QDs emit blue light, with other colours appearing between red and blue light. This phenomenon of colour changes shows that the variation of QDs particle size have certain optoelectronic properties and differ in their band gap energy (Yi 2013; Badawi et al. 2014). Band gap is the energy required for electrons to move and enter the excited state. Theoretically, small-sized QDs have larger band gap and require the same or higher energy than their band gap to enter excited state. Size tuning, energy levels and emission wavelengths of QDs make them extremely useful for some optoelectronic applications including photovoltaic cells (Kamat 2013) (Chang et al. 2013) (Hod and Zaban 2014), medical imaging (Wu et al. 2014), and sensors (Li et al. 2015) (Mozafari and Moztarzadeh 2011).

Basically, QDSSC consist of three important components which includes a photoelectrode sensitized with QDs, an electrolyte with a redox couple, and a counter electrode, as shown in Figure 1 (Mohamed Mustakim et al. 2018). Interestingly, QDs material have received considerable attention in the development of solar cell technology due to the effects of quantum confinement following the reduction in Bohr radius. The radius of Bohr's radius is the distance in the electron-hole pair which is different for each QDs material. QDs with smaller size than the Bohr radius are referred as strong quantum confinement effect, while QDs with larger size than Bohr radius are considered to be weak quantum confinement effect.

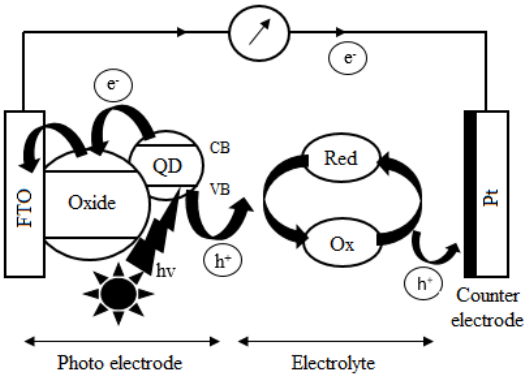

FIGURE 1. Operating principle of a typical QDSSC

As mentioned earlier, the electronic properties of QDs are determined by the size and shape that make them unique to the technology of today (Kamat 2013). In addition, photo stability and high absorption coefficients of QDs material can enhance the overall efficiency of solar cells devices. Multiple exciton generation (MEG) phenomenon is also a highly desirable feature of QDs especially in photovoltaic applications (Jun, Careem, and Arof 2013). The low cost of fabrication and production costs are also the benefits and advantages of QDSSCs.

Semiconductors such as cadmium sulphide (CdS), cadmium selenide (CdSe) and lead sulphide (PbS) have become the most popular options to be used to investigate the operating principles of QDSSCs. However, these materials are very toxicity that is seriously harmful to the environment (Z. A. Peng and Peng 2001). To overcome this issue, the development of eco-friendly QDs is very important for clean and safe QDSSCs future. $CuInS_2$ is a I-II-VI semiconductor material with direct energy gap of 1.5 eV (bulk) which is well matched with the full solar spectrum (Tell, Shay, and Kasper 1971) (Nanu, Schoonman, and Goossens 2005). It has many favorable features such as low cost, non-toxicity, high absorption coefficient and stable performance (Zhou et al. 2012). Theoretically, as the Bohr exciton radius of $CuInS_2$ is 4.1 nm, the quantum confinement effects can be observed in the nanoparticle up to size of about 8 nm (Kolny-Olesiak and Weller 2013). By controlling the sizes of $CuInS_2$ nanoparticles, their energy gap can be controlled as well as the absorption that can be tuned almost in the whole visible region of the solar spectrum, up to the near infrared.

Typically, larger particle size can lead to a narrower gap and the absorption edge gradually red-shifted to the higher wavelength (Liu et al. 2016) (Z. Peng et al. 2014). In general, the absorption spectrum of $CuInS_2$ does not show sharp peaks, but rather shows shoulder peaks. This could be attributed to the intrinsic nature of $CuInS_2$ itself or due to the size, shape or composition of the material in the sample studied. Thera are few methods can be used to synthesize the $CuInS_2$ QDs such as chemical bath deposition (CBD), solvothermal, successive ionic layer adsorption and reaction (SILAR), sol gel and more (Ward 2016).

To the best knowledge, this is the first investigation of QDSSCs performance with the effect of $CuInS_2$ QDs as sensitizer using Ag_2S as the passivation layers. Therefore, the main purpose of the current study is to explore the influence of different reaction times of solvothermal technique on the morphology, optical and electrical properties of nanostructured $CuInS_2$ QDs as an effective photosensitizer in solar cell. From this study, the optimum performance of environment friendly $CuInS_2$ QDs sensitizer can be used for further investigation on the effect of Ag_2S passivation layers towards the performance of $CuInS_2$ QDs based solar cells.

METHODOLOGY

Materials

TiO_2 P25 powder (99.5%; Sigma Aldrich), Acethylacethone (99%; Sigma Aldrich), Triton X-100 (Sigma Aldrich), Copper (II) Acetate monohydrate (99%; Merck), Indium Acetate (99.99%; Sigma Aldrich), Octadecylamine (90%; Merck), Thiourea (99%; Sigma Aldrich), Iodolyte AN-50 (Sigma Aldrich), ethanol, and acetone.

Characterization techniques

Morphology analysis was done using TEM (Philips model CM12) and Roughness measurements were carried out using AFM (Nanosuft Easyscan model). Structural analysis was done using XRD (Bruker AXS Germany model D8) with Cu-K_α radiation of wavelength, 1.5406 nm. Optical absorption studies were carried out with UV-Vis spectrophotometer (Perkin Elmer model Lambda 35). Illuminated J-V characteristics of the cells were measured with the help of Keithley source measure unit and the cells were illuminated using a xenon lamp with an intensity 100 mW/cm^2.

Preparation of TiO_2 photoelectrode

The Fluorine doped tin oxide (FTO) coated glass was used as a substrate in this experiment. The substrates were cleaned with 1:1:1 volume ratio of acetone, ethanol, and deionized water (DI water) and finally cleaned ultrasonically for 30 minutes. The TiO_2 thin films were prepared by using similar procedures by Feng et al. (2009). Briefly, 0.5 g of TiO_2 P25 powder was dispersed in 5 mL ethanol. The dispersion was grinded for several minutes followed by an addition of 0.05 mL acethy acetone. 0.05 mL Triton 100-X was added into the mixture to facilitate the spreading of the paste on the substrate, since this substance has the ability to reduce surface

tension, resulting in even spreading and reducing the formation of cracks (Badawi et al. 2015). Then, the prepared TiO_2 paste were spread onto cleaned FTO glass using the Doctor Blade method. Lastly, the glass substrate sintered at 450 °C for 30 minutes.

Preparation of $CuInS_2$ QDs

$CuInS_2$ QDs samples were prepared using modified solvothermal method by Yue et al. (2014). At room temperature, 0.05 mmol Cu $(Ac)_2{\cdot}H_2O$ was dispersed in 50 mL of absolute ethanol and stirred vigorously until a blue solution appeared. Then, 0.05 mmol In $(Ac)_3$ was added into the blue solution followed by dispersion of 0.60 mmol octadecylamine. The mixture solution was treated ultrasonically for several minutes, resulting in a sapphire colored dispersion. Addition of 0.20 mmol of $CS(NH_2)_2$ into the dispersion resulting a brown colored dispersion. The final brown dispersion was then transferred into a 40 mL capacity (~80%) of Teflon lined stainless steel autoclave and was heated up to 160°C for particular reaction times (t=2h, 4h, 6h and 8h). The autoclave was cooled down naturally to room temperature. Finally, the product was centrifuged (10,000 rpm, 8 minutes) and washed with absolute ethanol for 6 times. The product was then dried under N_2 environment at 60°C for 3 hours to other measurements.

Preparation of TiO_2/ $CuInS_2$ QDs thin films

The TiO_2 photo anode was place at an angle against the wall of the Teflon liner with the conductive side facing down. The prepared $CuInS_2$ precursor was transferred into an autoclave and was heated up to 160°C for different reaction times (t=2h, 4h, 6h and 8h). The autoclave was then cooled down naturally to room temperature. Finally, TiO_2/ $CuInS_2$ QDs thin films were rinsed by ethanol then dried at 60◦C under N_2 environment for 3 hours.

RESULTS AND DISCUSSION

Morphological properties

$CuInS_2$ nanoparticles were synthesized at temperature 160°C with different solvothermal reaction times. The prepared $CuInS_2$ affirmed by TEM images as shown in Figure 2 and the QDs size were determined using TEM measurement. From the result, the $CuInS_2$ could be called as QDs since the nanoparticles are smaller than 10 nm (Kouhnavard et al. 2014). The $CuInS_2$ QDs diameter are increasing from ±3.19 nm to ±8.67 nm with longer reaction time of 2 hours to 8 hours, respectively, as stated in Table 1. As observed, the $CuInS_2$ QDs are quasi-spherical and it aggregates to form QDs rich domains by the individual QDs particles.

TABLE 1. The physical properties of diameter of $CuInS_2$ QDs with different solvothermal reaction times

Samples	Diameter [nm]	Roughness [nm]
$CuInS_2$ 2h	±3.19	6.82
$CuInS_2$ 4h	±5.88	12.63
$CuInS_2$ 6h	±6.45	17.80
$CuInS_2$ 8h	±8.67	16.61

The root mean square (RMS) analysis has been carried out using AFM to characterize the surface roughness of TiO_2/ $CuInS_2$ QDs thin films. From Figure 3, it is noticeable that the value of RMS increases from 6.82 nm to 17.80 nm with longer reaction time of 2 hours to 6 hours, respectively, as stated in Table 1. However, the RMS of the thin film shows a relatively smoother surface when it reaches 8 hours reaction. This could be attributed to the growth of $CuInS_2$ that have larger particles size than other samples, effecting the roughness reduction (A.Al-Khafaji et al. 2016).

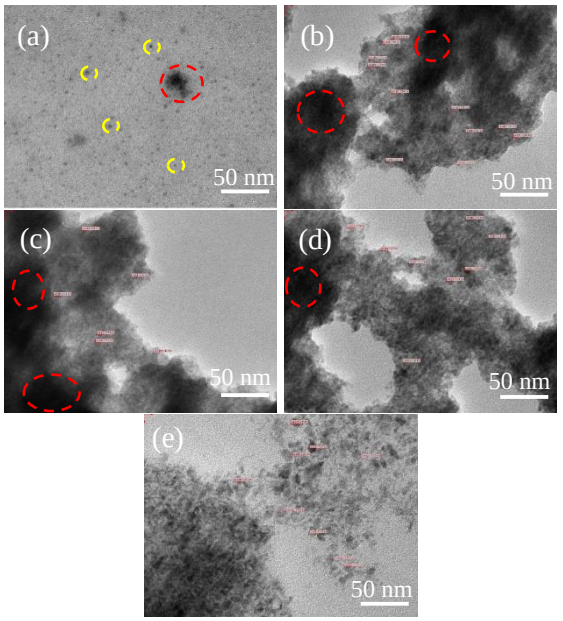

FIGURE 2. TEM images of $CuInS_2$ QDs with different solvothermal reaction times (a - b) 2 hours (c) 4 hours (d) 6 hours and (e) 8 hours; the yellow dashed lines identify the quasi-spherical individual QDs, while the red dashed lines identify the QDs rich domains

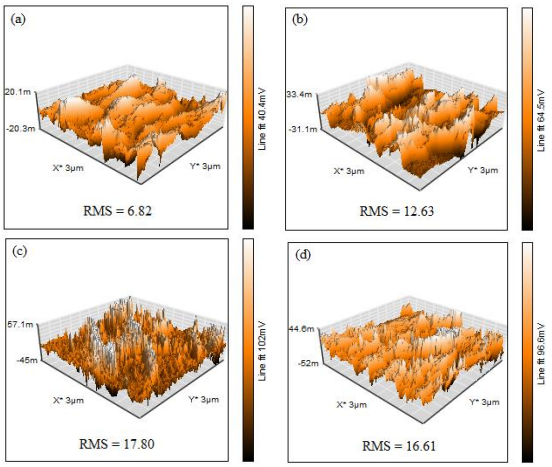

FIGURE 3. AFM images of $CuInS_2$ QDs with different solvothermal reaction times (a) 2 hours (b) 4 hours (c) 6 hours and (d) 8 hours

Structural properties

XRD analysis were carried out to further identify the phase composition and phase structure of prepared $CuInS_2$ QDs. Figure 4 displays the X-ray diffraction patterns that consists of three major peaks at 27.9°, 46.3° and 54.9° which in good agreement with crystal faces (112), (204) or (220) and (116) or (312)

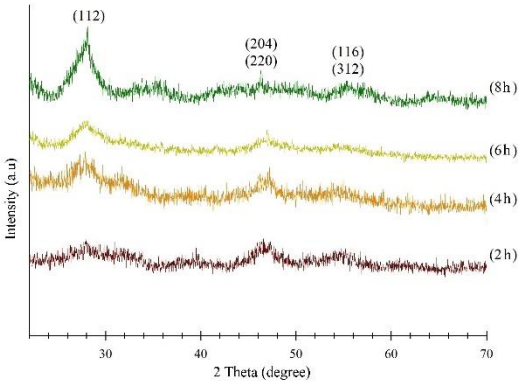

FIGURE 4. XRD spectra of $CuInS_2$ QDs with different solvothermal reaction times

of tetragonal $CuInS_2$ structure (PDF 03-065-2732). These peaks are just relatively broad which indicating small crystalline $CuInS_2$ particles. The crystallite size of $CuInS_2$ QDs was estimated to be approximately 3.69 nm, 5.64 nm, 6.19 nm, and 7.52 nm with different reaction times of 2 hours, 4 hours, 6 hours, and 8 hours, respectively, by Scherrer's equation (1). The values obtained is consistent with that observed in TEM images.

TABLE 2. The calculated crystallite size $CuInS_2$ QDs with different solvothermal reaction times using Scherrer's equation

Sample	Position 2θ [deg.]	FWHM [deg.]	Crystallite size [nm]
$CuInS_2$_2h	27.945	2.435	3.693
$CuInS_2$_4h	27.858	1.595	5.641
$CuInS_2$_6h	28.121	1.454	6.189
$CuInS_2$_8h	28.115	1.198	7.522

$$d = \frac{k\lambda}{\beta \cos\theta} \quad (1)$$

From the calculation, k is the shape constant (0.9), λ is the wavelength of the X-ray (0.15406 nm), β is the FWHM in radians and θ is the Bragg's angle in degrees. It is observed that there is an increment of crystallite size with longer reaction times as stated in Table 2.

Optical properties

From the absorption spectra, the light harvesting range of $CuInS_2$ QDs covers the whole visible spectrum and could extends to NIR region with long wavelength direction typically up to 900 nm (Yue et al. 2013). Therefore, the energy gap can be tuned between 3.3 eV and 1.7 eV. Figure 5 shows an enhancement in the optical absorbance and slightly red shifted at the absorption edge as the reaction time extended. This is obviously because of the increase in QDs particle size that would lead in the increased absorbance thus influencing the energy gap.

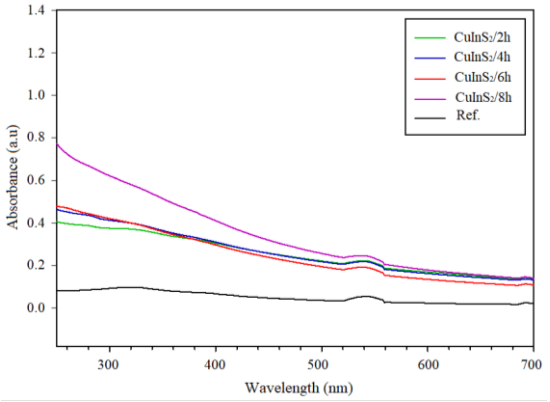

FIGURE 5. UV-VIS absorption spectra of $CuInS_2$ QDs with various reaction times

The energy gap of prepared $CuInS_2$ QDs was estimated using Tauc plot. As stated in Table 3, the energy gap for prepared $CuInS_2$ QDs is between 2.16 eV and 2.02 eV which are found to gradually

narrower with bigger size of QDs. This can be attributed to the QDs effect (Yue et al. 2014). In other words, larger $CuInS_2$ QDs with smaller energy gap helps for better absorbance, thus contributing to better and stronger light harvesting ability.

TABLE 3. Determination of band gap energy of $CuInS_2$ QDs at different solvothermal reaction times

Samples	Bandgap energy[eV]
$CuInS_2$ 2h	2.16
$CuInS_2$ 4h	2.14
$CuInS_2$ 6h	2.10
$CuInS_2$ 8h	2.02

Electrical properties

The photocurrent density-voltage (J-V) curves were measured under the irradiation (E) of the simulated sunlight (100 mW/cm^2) to confirm the influence of different solvothermal reaction times on the photovoltaic performance, as shown Figure 6. To undergo the J-V test, the QDSSCs were fabricated as a sandwich type cell with active area (A_C) of 0.25 cm^2.

The TiO_2/$CuInS_2$ thin film was used as the photo anodes and platinum as the counter electrodes by using a thin transparent surlyn ring to inject the commercial iodine-based electrolyte (Iodolyte AN-50). Four different sets (t = 2h, 4h, 6h ,8h) of sandwiched-type solar cell were prepared to determine the device efficiency. The following equations (2) and (3) express conversion efficiency:

$$Pmax = FF * Voc * Isc \quad (2)$$

$$\eta = \frac{Pmax}{E * Ac} \quad (3)$$

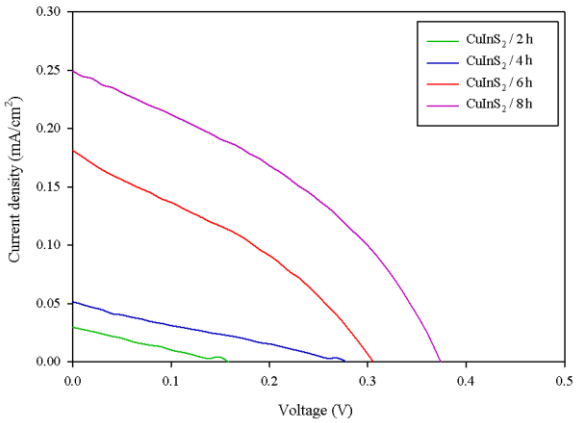

FIGURE 6. J-V curves of $CuInS_2$ based QDSSCs with different solvothermal reaction times

Based on these curves, the power conversion efficiency of the samples gradually increases with longer solvothermal reaction time, as listed in Table 4. The result shows the best efficiency of 0.035% with 8 hours reaction time. As can be seen that the value of short circuit current (I_{sc}) was significantly improved from 0.030 mA/cm^2 to 0.249 mA/cm^2 as the reaction time was prolonged from 2 hours to 8 hours. However, it should be noticed that the power conversion efficiency of $CuInS_2$ based QDSSCs present in our study is still low. This may be due to the limitation of the lattice mismatch between TiO_2 and $CuInS_2$ QDs and high surface state density that exist in the heterostructure of the layers which could lead in a high rate of interface recombination (Zhou et al. 2012). Therefore, a study on the band alignment of TiO_2 and $CuInS_2$ QDs should be conducted for better QDSSCs performance.

TABLE 4. The conversion efficiency of $CuInS_2$ QDs with different solvothermal reaction times

Sample	V_{oc} (V)	I_{sc} (A)	FF (%)	P_{max} (W)	Ƞ (%)
$CuInS_2$ 2h	0.158	0.030	24	2.80 x 10^{-7}	0.001
$CuInS_2$ 4h	0.277	0.051	25	8.90 x 10^{-7}	0.004
$CuInS_2$ 6h	0.305	0.181	33	4.56 x 10^{-6}	0.018
$CuInS_2$ 8h	0.374	0.249	37	8.63 x 10^{-6}	0.035

CONCLUSION

From the study, $CuInS_2$ QDs ranged of $\pm$3.19 nm to $\pm$8.67 nm has been successfully prepared with different solvothermal reaction times. The effect of reaction times on the photovoltaic performance of $CuInS_2$ based QDSSCs was investigated. From XRD result, there are peaks at 27.9°, 46.3° and 54.9° of tetragonal $CuInS_2$ structure. The broad peaks of this material indicating small crystallite size which corresponding to the $CuInS_2$ size obtained from TEM analysis. According to UV-VIS result, there is a small red shift of absorption edge as well as an enhancement in the optical absorbance. The energy gap of $CuInS_2$ QDs can also be determined which resulting in narrower gap with increased absorbance. Lastly, the efficiency of the solar cells keeps increasing as the reaction time increased. The objective of this study was achieved by obtaining the highest conversion efficiency of 0.035% when the reaction time increased up to 8 hours. Therefore, the 8 hours $CuInS_2$ QDs should be used for further investigation on the effect of Ag_2S passivation layer towards the $CuInS_2$ QDs based solar cell performance.

ACKNOWLEDGEMENT

The authors would like to thank the financial assistance provided by Ministry of Energy, Science, Technology, Environment and Climate Change (MESTECC). Besides, the authors are thankful to the supports received from Center for Research and Instrumentation Management (CRIM) and Solar Energy Research Institute (SERI) in The National University of Malaysia (UKM).

REFERENCES

A.Al-Khafaji, Abdul Kareem, Dheyaa B.Alwan, Falah H.Ali, and Wesam A.A.Twej. 2016. "Influence of Grain Size, Electrode Type and Additives on Dye Sensitized Solar Cells Efficiency." *Environment Science* 12 (6): 217–23.

Badawi, Ali, N. Al-Hosiny, and S. Abdallah. 2015. "The Photovoltaic Performance of CdS Quantum Dots Sensitized Solar Cell Using Graphene/TiO_2 Working Electrode." *Superlattices and Microstructures* 81: 88–96.

Chang, C C, J K Chen, C P Chen, C H Yang, and J Y Chang. 2013. "Synthesis of Eco-Friendly $CuInS_2$ Quantum Dot-Sensitized Solar Cells by a Combined Ex Situ/in Situ Growth Approach." *ACS Appl Mater Interfaces* 5 (21): 11296–306.

Feng, Jiamin, Jianjun Han, and Xiujian Zhao. 2009. "Synthesis of $CuInS_2$ Quantum Dots on TiO_2 Porous Films by Solvothermal Method for Absorption Layer of Solar Cells." *Progress in Organic Coatings* 64 (2–3): 268–73.

Hegazy, Maroof A, and Afaf M Abd El-hameed. 2014. "Characterization of CdSe-Nanocrystals Used in Semiconductors for Aerospace Applications : Production and Optical Properties." *NRIAG Journal of Astronomy and Geophysics* 3 (1): 82–87.

Hod, Idan, and Arie Zaban. 2014. "Materials and Interfaces in Quantum Dot Sensitized Solar Cells: Challenges, Advances and Prospects." *Langmuir : The ACS Journal of Surfaces and Colloids* 30 (25): 7264–73.

Jun, H. K., M. A. Careem, and A. K. Arof. 2013. "Quantum Dot-Sensitized Solar Cells-Perspective and Recent Developments: A Review of Cd Chalcogenide Quantum Dots as Sensitizers." *Renewable and Sustainable Energy Reviews* 22: 148–67.

Kamat, Prashant V Pv. 2013. "Quantum Dot Solar Cells . The Next Big Thing in Photovoltaics." *The Journal of Physical Chemistry Letters* 4: 908–18.

Kolny-Olesiak, Joanna, and Horst Weller. 2013. "Synthesis and Application of Colloidal $CuInS_2$ Semiconductor Nanocrystals." *ACS Applied Materials & Interfaces* 5: 12221–37.

Kouhnavard, M., S. Ikeda, N. A. Ludin, N. B. Ahmad Khairudin, B. V. Ghaffari, M. A. Mat-Teridi, M. A. Ibrahim, S. Sepeai, and K. Sopian. 2014. "A Review of Semiconductor Materials as Sensitizers for Quantum Dot-Sensitized Solar Cells." *Renewable and Sustainable Energy Reviews* 37: 397–407..

Li, Zhuo, Yong Wang, Yongnian Ni, and Serge Kokot. 2015. "A Sensor Based on Blue Luminescent Graphene Quantum Dots for Analysis of a Common Explosive Substance and an Industrial Intermediate, 2,4,6-Trinitrophenol." *Spectrochimica Acta - Part A: Molecular and Biomolecular Spectroscopy* 137: 1213–21.

Liu, Yueli, Tao Chen, Zhuoyin Peng, Lei Wu, Keqiang Chen, Peng Zhou, Linlin Wang, and Wen Chen. 2016. "Size-Dependent Photoluminescence Dynamics of $CuInS_2$ Quantum Dots and Charge Injection on Titanium Oxide Film." *Journal of Alloys and Compounds* 658: 76–84.

Mohamed Mustakim, Nurul Syafiqah, Charles Ahamefula Ubani, Suhaila Sepeai, Norasikin Ahmad Ludin, Mohd Asri Mat Teridi, and Mohd Adib Ibrahim. 2018. "Quantum Dots Processed by SILAR for Solar Cell Applications." *Solar Energy* 163 (September 2017): 256–70.

Mozafari, M., and F. Moztarzadeh. 2011. "Microstructural and Optical Properties of Spherical Lead Sulphide Quantum Dots-Based Optical Sensors." *Micro & Nano Letters* 6 (3): 161.

Nanu, Marian, Joop Schoonman, and Albert

Goossens. 2005. “Solar-Energy Conversion in TiO_2 / $CuInS_2$ Nanocomposites.” *Advanced Functional Materials* 15 (1): 95–100.

Peng, Z. A., and X. Peng. 2001. “Formation of High-Quality CdTe, CdSe, and CdS Nanocrystals Using CdO as Precursor [6].” *Journal of the American Chemical Society* 123 (1): 183–84..

Peng, Zhuoyin, Yueli Liu, Keqiang Chen, Guojie Yang, and Wen Chen. 2014. “Fabrication of the Protonated Pentatitanate Nanobelts Sensitized with $CuInS_2$ Quantum Dots for Photovoltaic Applications.” *Chemical Engineering Journal* 244: 335–42.

Tell, B., J. L. Shay, and H. M. Kasper. 1971. “Electrical Properties, Optical Properties, and Band Structure of $CuGaS_2$ and $CulnS_2$.” *Physical Review B* 4 (8): 2463–71.

Ward, Harrison. 2016. “Copper Indium Sulfide Quantum Dots for Light Selective Nanocomposite Thin Films and Solar Cell Applications,” no. January.

Wu, Pei-jung, Keng-liang Ou, Jem-kun Chen, and Hsiao-ping Fang. 2014. “Methotrexate-Conjugated $AgInS_2$ / ZnS Quantum Dots for Optical Imaging and Drug Delivery.” *Materials Letters* 128: 412–16.

Yue, Wenjin, Mingyang Lan, Guoqiang Zhang, Wenshan Sun, Songming Wang, and Guangjun Nie. 2014. “Size-Dependent Polymer/$CuInS_2$ Solar Cells with Tunable Synthesis of $CuInS_2$ CVGJFHYK []Q; Quantum DotsY’P.” *Materials Science in Semiconductor Processing* 24: 117–25..

Yue, Wenjin, Fan Wu, Changwen Liu, Zeliang Qiu, Qi Cui, Hui Zhang, Feng Gao, Wei Shen, Qiquan Qiao, and Mingtai Wang. 2013. “Incorporating $CuInS_2$ Quantum Dots into Polymer/Oxide-Nanoarray System for Efficient Hybrid Solar Cells.” *Solar Energy Materials and Solar Cells* 114: 43–53.

Zhou, Zhengji, Shengjie Yuan, Junqi Fan, Zeliang Hou, Wenhui Zhou, Zuliang Du, and Sixin Wu. 2012. “$CuInS_2$ Quantum Dot-Sensitized TiO_2 Nanorod Array Photoelectrodes: Synthesis and Performance Optimization.” *Nanoscale Research Letters* 7 (1): 652.